Structural aspects of AlPO$_4$-5 zeotypes synthesized by microwave-hydrothermal process. 1. Effect of heating time and microwave power

Billur Sakintuna · Yuda Yürüm

Abstract AlPO4-5 with AFI structure containing 12-membered rings was prepared using the aluminum isopropoxide precursor as a source of alumina and TEA as the structure directing agent via microwave technique. The influence of microwave power and heating time on the dimensions of AlPO$_4$-5 crystals formed in the system Al$_2$O$_3$:P$_2$O$_5$:(C$_2$H$_5$)$_3$N (or (C$_3$H$_7$)$_3$N):H$_2$O:HF has been studied systematically. It was found that the morphology of the AlPO$_4$-5 depended on the microwave power and heating time. Several mechanisms of fast crystallization existed in the microwave radiation, due to increased dissolution of the gel by lonely water molecules in almost temperature gradient-free and convection-free in situ heating.

1 Introduction

Porous materials with pore sizes near molecular dimensions, such as zeolites and aluminophosphate molecular sieves (AlPO), have been widely used in catalysis [1] and separation, and development for new applications in membranes, sensors, optics, etc., is in progress [2]. These new materials comprise a series of crystalline, microporous aluminophosphates (AlPOs) hydrothermally prepared from reaction mixtures containing inorganic sources of Al and P and an organic template (such as amine or a quaternary ammonium salt). These materials present strict alternation of AlO$_4^-$ and PO$_4^+$ tetrahedrons with a neutral framework [3–6].

The aluminophosphates are usually synthesized using thermal heating conditions with a reaction time ranging from several hours to several days. It is known that the AFI type can be prepared utilizing several structure-directing agents; for example TEA, TEAOH, TPA, TPAOH and TBAOH. A new synthesis method using microwave heating has been employed for the preparation of microporous AlPO4-5 zeotype due to a reduction of the crystallization time. The microwave-assisted synthesis of molecular sieves is a relatively new area of research. It offers many distinct advantages over conventional synthesis. They include rapid heating to crystallization temperature due to volumetric heating, resulting in homogeneous nucleation, fast supersaturation by the rapid dissolution of precipitated gels and eventually a shorter crystallization time compared to conventional autoclave heating. It is also energy efficient and economical. This method has been successfully applied and reviewed for the synthesis of several types of zeolites namely zeolite A, Y, ZSM-5, MCM-41, metal substituted aluminophosphate, silico-aluminophosphate and gallophosphate [7–9].

Microwave-assisted heating is known to be able to accelerate the nucleation, thus results in fast crystallization [9–11] as well as products with high purity and narrow particle size distribution [12]. Microwave irradiation is more efficient for transferring thermal energy to a volume of material than conventional thermal processing which transfers heat to the material by convection, conduction and radiation. Microwave technique has been widely applied in the synthesis of the zeolite and molecular sieves because of the reduced reaction time and improved crystal quality. Microwave technique offers more rapid

B. Sakintuna · Y. Yürüm (✉)
Faculty of Engineering and Natural Sciences, Sabanci University, Orhanli, Tuzla, Istanbul 34956, Turkey
e-mail: yyurum@sabanciuniv.edu

crystallization than conventional hydrothermal method and it is believed more nuclei are generated simultaneously, thus the growth of the crystals is homogeneous [13, 14]. Some research groups have reported the morphology control of porous materials such as VSB-5 [15] and SBA-16 [16] under microwave irradiation and have showed the microwave is a very efficient tool to control the morphology of porous materials.

In the present report by utilizing microwave techniques, we present the synthesis of AlPO$_4$-5 zeotypes with various morphologies such as aggregated sphere, plate, rod and aggregated faggot. The effects of microwave power and heating time on the morphology were investigated and explained by the combined results of XRD and SEM.

2 Experimental

2.1 Synthesis

The preparation details of AlPO$_4$-5 crystallization using different initial solutions and conditions of hydrothermal crystallization using a domestic microwave oven are as follow. The reactants were phosphoric acid (H$_3$PO$_4$ 85 wt%), aluminum isopropoxide (C$_9$H$_{21}$O$_3$Al, 99.9%, triethylamine (TEA, 99.5%) (C$_2$H$_5$)$_3$N and hydrofluoric acid (HF, 40 wt%). The sample that contained the AlPO$_4$-5 crystals was prepared from the starting mixture with the molar compositions given in Table 1. Aluminum isopropoxide was first hydrolyzed in deionized water, and H$_3$PO$_4$ was added. TEA added to the mixture dropwise into the reaction mixture while stirring. After the addition of HF, the gel was aged at room temperature for 2 h. The suspension was transferred into a cylindrical (7 cm outer diameter and 18 cm height) Teflon autoclave of 130 mL internal volume. The cap of the autoclave was closed tightly to prevent any leakage of the chemicals in the autoclave and the autoclave was placed in a Delonghi EMD MW 311 model microwave oven according to the experimental parameters given in Table 1. The microwave oven operated at 230 V, 50 Hz, maximum microwave power output of the oven was 800 W. After the synthesis, the autoclave was cooled to room temperature. All products were filtrated, washed with distilled water several times and dried in an oven at 383 K for 5 h. Yield of the experiments were nearly stoichiometric with respect to the alumina and phosphate ingredients added to the synthesis mixture. The product was washed and dried, followed by calcining at 600 °C for 7 h.

2.2 Characterization

The crystal structure and crystallinity of the samples were analyzed by powder X-ray diffraction with a Bruker axs advance powder diffractometer fitted with a Siemens X-ray

Table 1 Parameters of the microwave synthesis of AlPO$_4$-5's (samples H)

Sample name	Molar gel composition						Mode of heating			
	Al$_2$O$_3$	P$_2$O$_5$	TPA	TEA	HF	H$_2$O	First step		Second step	
							Power (W)	Heating time (s)	Power, (W)	Heating time (s)
H1	1	1	–	1.3	1	70	120	300	–	–
H2	1	1	–	1.3	1	70	120	600	–	–
H3	1	1	–	1.3	1	70	120	900	–	–
H4	1	1	–	1.3	1	70	200	180	–	–
H5	1	1	–	1.3	1	70	200	240	–	–
H6	1	1	–	1.3	1	70	200	270	–	–
H7	1	1	–	1.3	1	70	200	285	–	–
H8	1	1	–	1.3	1	70	200	300	–	–
H9	1	1	–	1.3	1	70	200	315	–	–
H10	1	1	–	1.3	1	70	200	330	–	–
H11	1	1	–	1.3	1	70	200	360	–	–
H12	1	1	–	1.3	1	70	200	420	–	–
H13	1	1	–	1.3	1	70	200	600	–	–
H14	1	1	–	1.3	1	70	200	900	–	–
H15	1	1	–	1.3	1	70	800	60	–	–
H16	1	1	–	1.3	1	70	800	60	120	300
H17	1	1	–	1.3	1	70	800	60	120	600
H18	1	1	–	1.3	1	70	800	60	200	300

gun and equipped with Bruker axs Diffrac PLUS software using CuKα radiation. The sample was rotated (20 rpm) and swept from $2\theta = 5°$ through to $80°$ using default parameters of the program. The X-ray generator was set to 40 kV at 40 mA. All the XRD measurements were repeated at least three times and the results reported were the average of these measurements. The XRD patterns of the samples indicate their high level of crystallinity. The degree of crystallinity was estimated by summing the areas of the five major diffraction peaks. The structure and morphology of the AlPO$_4$-5 molecular sieves depend on the gel composition and heating periods. The phase purity is also dependent on the composition of the gels. All synthesis batches produced nearly identical fractions of AlPO$_4$-5, i.e., 0.1 g per 1 g of the gel.

The morphology of the products after coating with Au was examined with a Leo Supra 35VP Field emission scanning electron microscope, Leo 32 and electron dispersive spectrometer software was used for images and analysis. Imaging was generally done at 2–5 keV accelerating voltage, using the secondary electron imaging technique.

Surface area and pore analyses were performed with a Quantachrome NOVA 2200e Surface Area and Pore Size analyzer at 77 K. Before the experiment the samples were heated for 12 h at 120 °C and outgassed for 2 h at 350 °C. Surface area of the samples was determined by using Brunauer, Emmett and Teller (BET) method in the relative pressure range of between 0.05 and 0.25, over five adsorption points. Pore size distributions were calculated using Barrett, Joyner and Halenda (BJH) method.

3 Results and discussion

Effect of heating times on the morphology of AlPO$_4$-5 crystals were studied in H-labelled syntheses. Longer heating time during the syntheses did not have any effect on the morphology of the crystals formed. Increasing the microwave power did not also change the appearance of the crystals (Fig. 1a and b). Same type of crystals were obtained in H1 through H4 with some new nascent crystals in the surroundings. The perfect hexagonal prisms of AlPO$_4$-5 products with well-defined edges and faces formed in the microwave synthesis labelled as H1 and H4 are shown in Fig. 1. This shape is one of the characteristic morphologies of AlPO$_4$-5 crystals [17–19]. The direction of the *c*-axis is parallel to the six-fold axis of this rod-like shape. The *a*–*b* plane is perpendicular to the *c*-axis. The average crystal sizes in length along the *c*-axis were obtained ca. 10 μm length from the SEM images. XRD patterns of products labeled as H1, H2, H3 and H4 are presented in Fig. 2. The X-ray powder diffraction pattern
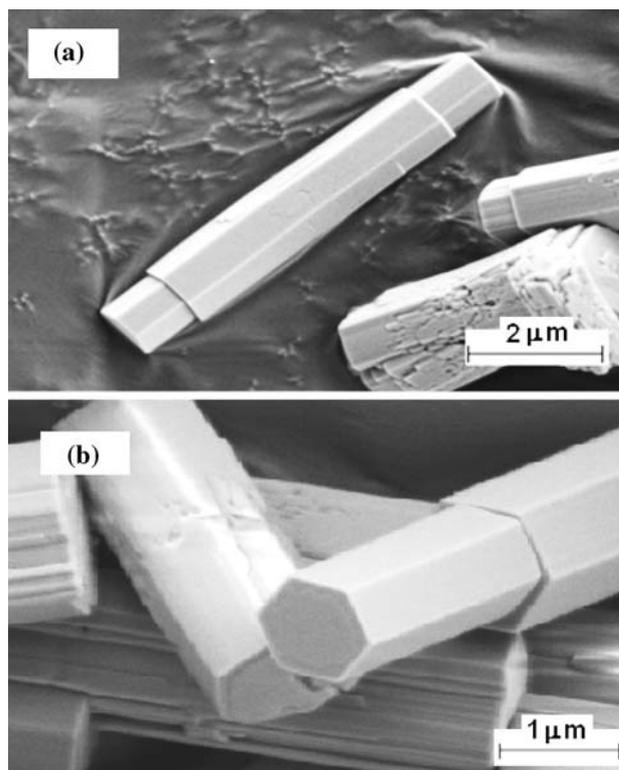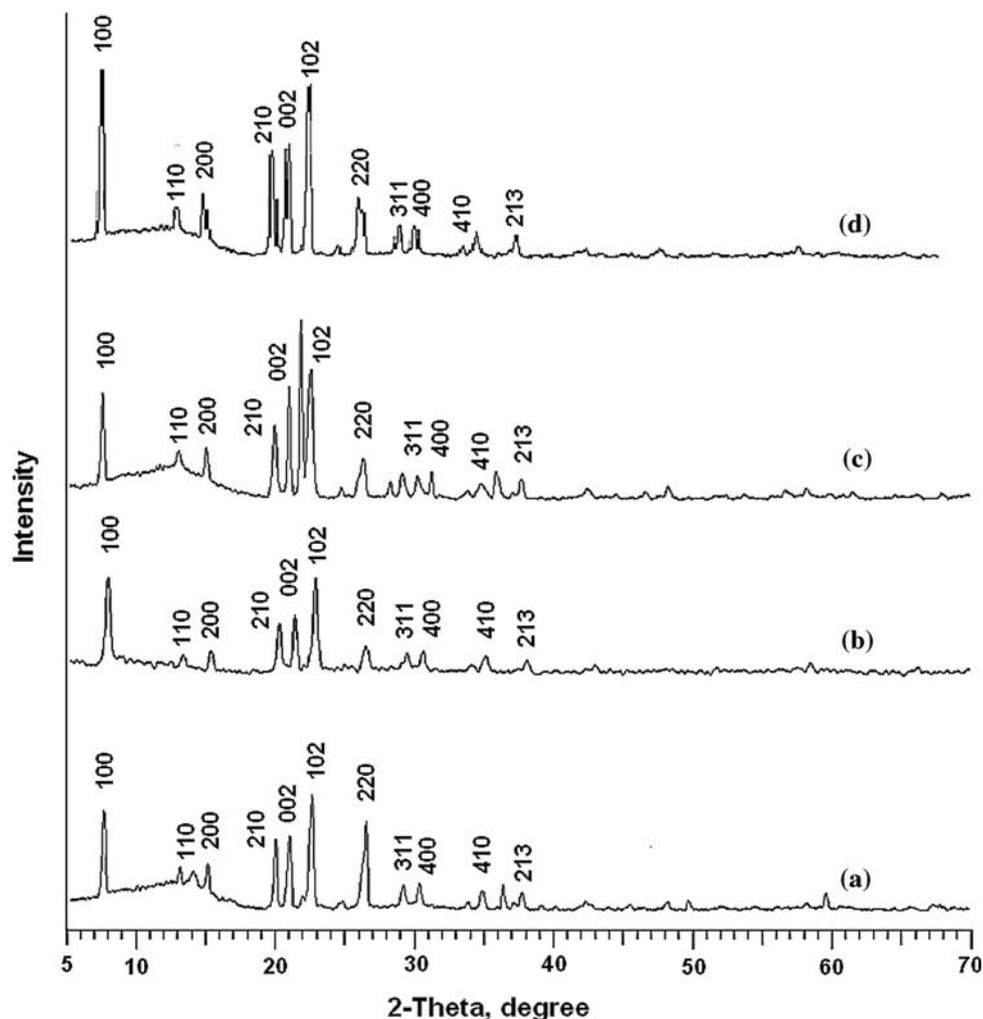

Fig. 1 SEM micrographs of **a** H1 (120 W, 300 s and **b** H4 (200 W, 180 s)

of the synthesized AlPO4-5 products indicated the presence of similar peaks of AFI structures that were published in the literature [11, 17, 20]. Diffraction patterns of both samples indicate their high level of crystallinity. The XRD patterns of AlPO$_4$-5 crystals of H1, H2, H3 and H4 contained the main peaks which characterized AFI structure, 100, 200, 210, 002, 102 and 220, were detected and in addition small features such as 110, 311, 400, 410 and 213 were also present.

Increasing the microwave power from 120 to 200 W, also resulted in perfect AlPO$_4$-5 crystals of ca. 5 μm length even at a shorter length of time of 180 s. SEM micrograph of H4 was shown in Fig. 1b. Both the appearance and XRD patterns of products H1 and H4 are similar with perfect AlPO$_4$-5 crystals published in the literature [21, 22]. The frameworks of products H1 and H4 were consistent with the AFI-structure type found in Qui et al. [17]. 4-, 6-, and 12-rings of the corner sharing PO$_4$ and AlO$_4$ tetrahedra were present. In H1 and H4, the formations of crystals nuclei were mostly homogeneous.

The pore size distribution and isotherm have type IV isotherm containing a hysteresis loop at relative pressures (P/P_0) higher than 0.4, representing mesoporous materials. BET surface area of H1 and H4 was 61 m^2/g (C = 58.1) and 107 m^2/g (C = 85.1), respectively. The BET "C" constants were within the accepted range of 20–200 for

zeolitic materials. The physisorption for all samples also gave similar results, corresponding to mesoporous materials (not shown). N_2 adsorption/desorption isotherms and pore size distributions of H1 and H4 were given in Figs. 3 and 4, respectively. Increasing the power from 120 to 200 W seemed to effect the porosity of the crystals formed, pore size distribution in the H4 crystals was narrower than that of H1 crystals. The reason for this might be the increased rate of crystallization in higher microwave power surroundings so that the crystals had more homogeneous porosity under such conditions. At low powers the gel might not be fully converted to crystals which led to the broad pore size distribution in Fig. 4a. This also coincided with the lower XRD intensity in Fig. 2a. Average pore diameters of H1 and H4 were measured as 2–10 and 2 nm, respectively, demonstrating presence of mesoporous framework. Utchariyajit and Wongkasemjit [23] also synthesized a mesoporous $AlPO_4$-5 (AFI) zeotype using alumatrane precursor.

SEM micrographs of H1 and H4 obtained at the 50 s of heating are shown in Fig. 5. Demuth et al. [24] reported that the nucleation occurred even during the heating to the set temperature. It could be concluded that the growing of the crystals began to form the hourglass orientation. It was shown that the $AlPO_4$-5 crystals, freely grown in solution, always consisted of two half-crystals with opposite growth direction along the c axis of the crystal. There are two alternatives to correlate the two half-crystals [25]. The first option is that the two halves of the AFI crystal are related by a 180° rotation about a diagonal in the hexagonal plane. Both half-crystals have the same absolute configuration. Another possibility is that the structures in the two half-crystals are related by a mirror plane or, equivalently, by inversion. Consequently, the two half-crystals have a different absolute structure. In both cases, the two end faces of a crystal are identical [25]. The end face of crystals, perpendicular to the main growth direction, terminated with Al atoms. Although $AlPO_4$-5 crystals are found to have twinned structure, the growth process has not yet been clarified [26]. Lin et al. [27] synthesized "dumbbell" or "half-dumbbell" shaped $AlPO_4$-5's. The central part of the crystal is a hexagonal prism. At the ends of the crystals,
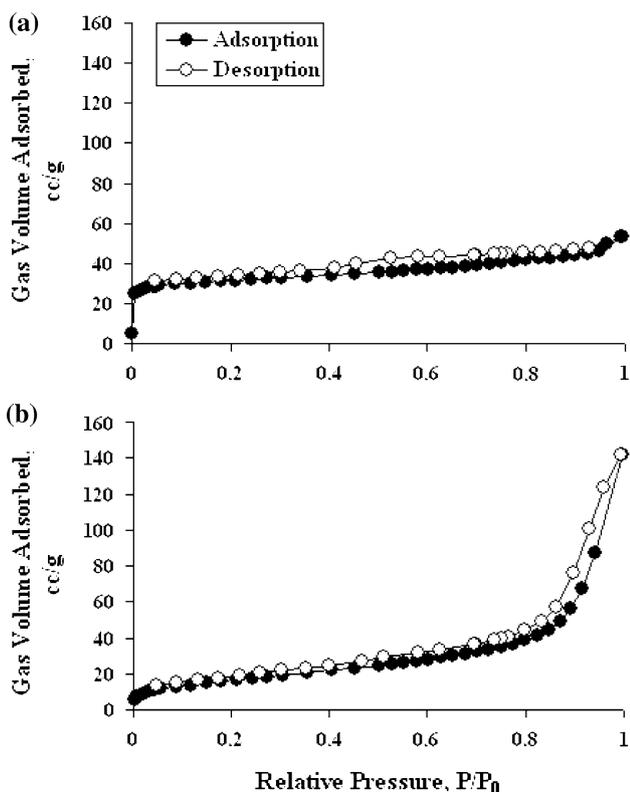
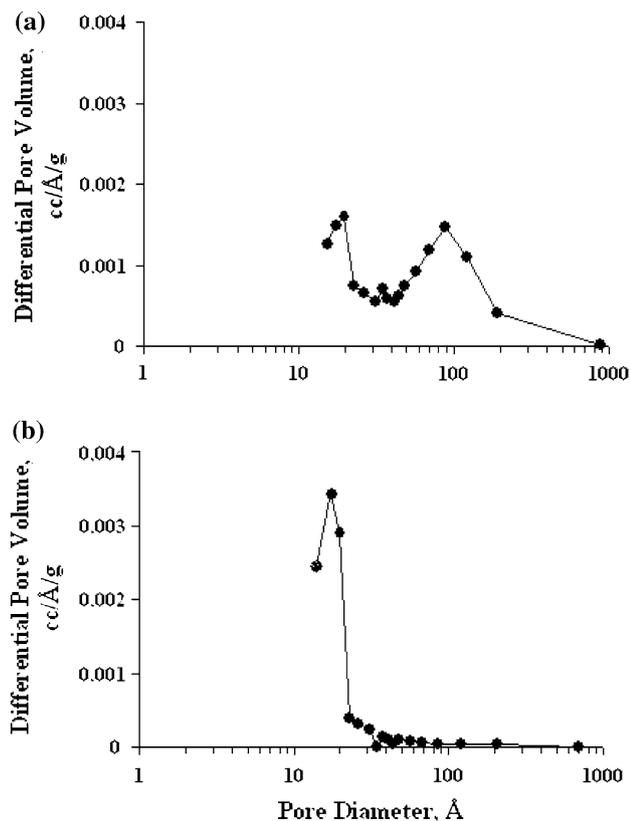Fig. 3 N$_2$ adsorption/desorption isotherms of **a** H1 and **b** H4

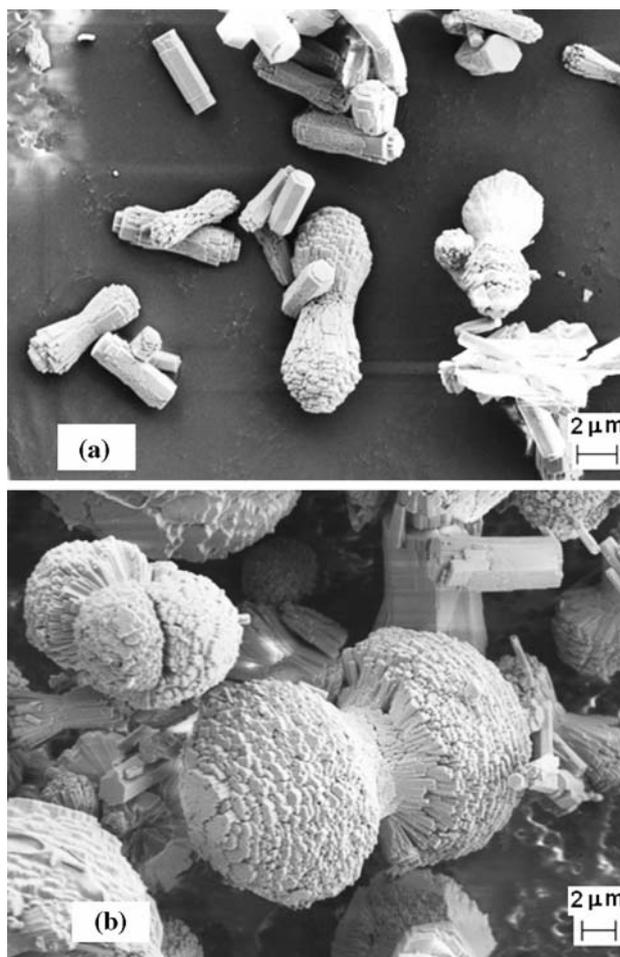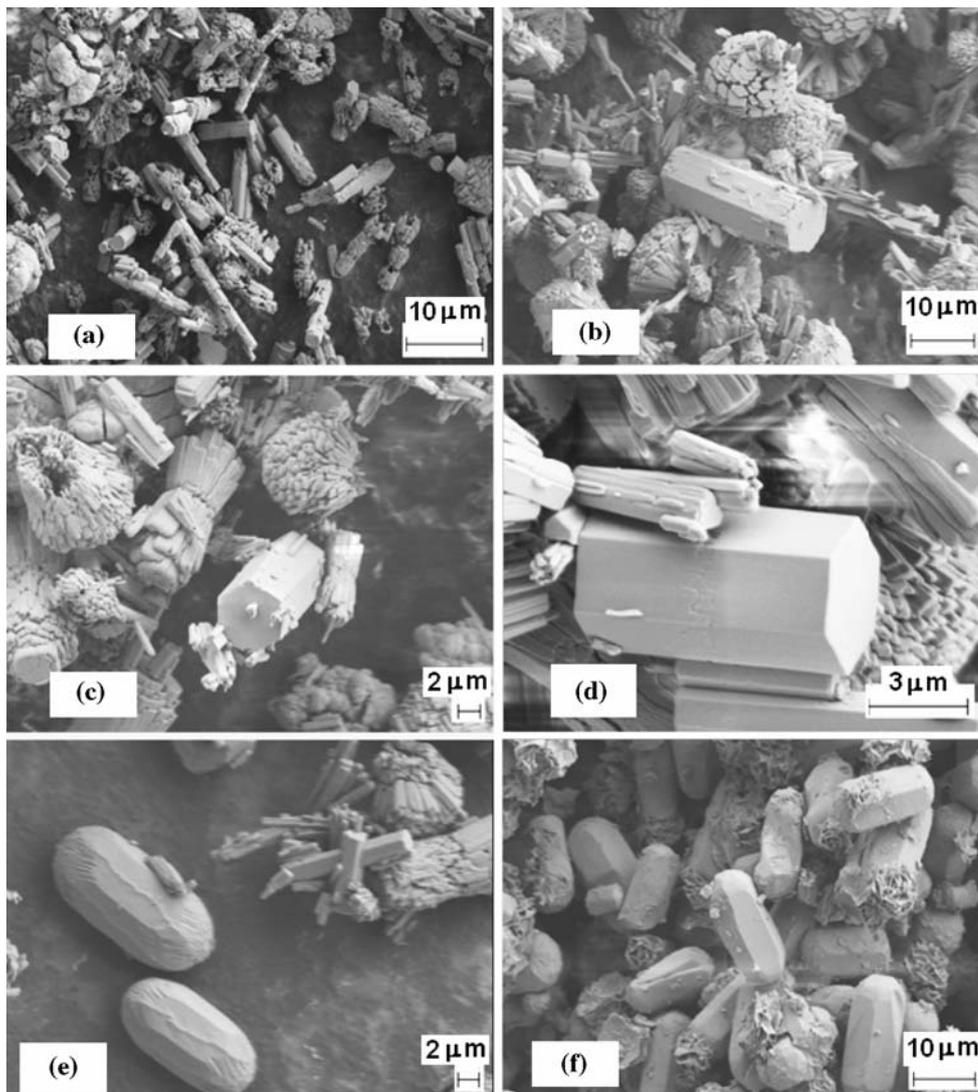Fig. 4 Pore size distributions of **a** H1 and **b** H4

Fig. 5 SEM micrographs of **a** H1 and **b** H4 obtained at the 50 s of heating

smaller twinned crystals radiate out from the central hexagonal part. Other researchers have observed dumbbell-shaped AlPO$_4$-5 crystals in traditional hydrothermal synthesis under certain conditions [28]. In the present study, crystals obtained belonged to hexagonal space group P6/mcc according to XRD patterns [17]. At longer heating periods dumbbell morphology converted to hexagonal crystals. The hexagonal unit cell parameters and volume are $a = 13.770$ Å, $c = 8.379$ Å, and $V = 1376.04$ Å^3.

Increasing the microwave power to 200 W and crystallization time to 240–300 s caused formation of hexagonal as well as hourglass shaped and conical crystals, in the samples labeled as in H5, H6, H7, H8, H9 and H10 (Fig. 6). With the increase in the microwave heating time to 240 s in H5, the crystals grown only in the c-axis direction and close to hexagonal rod-like shape with no size change in the a–b plane. Nucleation of the needle-like crystals were observed near the large crystals in H6, also observed in a previous study [26]. The AlPO$_4$-5 product of sample H9 and H10 transformed hexagonal crystals into

Fig. 6 SEM micrographs of **a** H5, **b** H6, **c** H7, **d** H8, **e** H9 and **f** H10

convex ended and angled surface. Increasing the crystallization time to 330 s, caused the formation of the conical crystals before transformed into larger amounts of hexagonal and convex ended crystals. Increasing the microwave heating times up to 315 and 330 s, in H9 and H10, respectively, brought about the crystals in H9 and H10 to grow in the *a–b* direction.
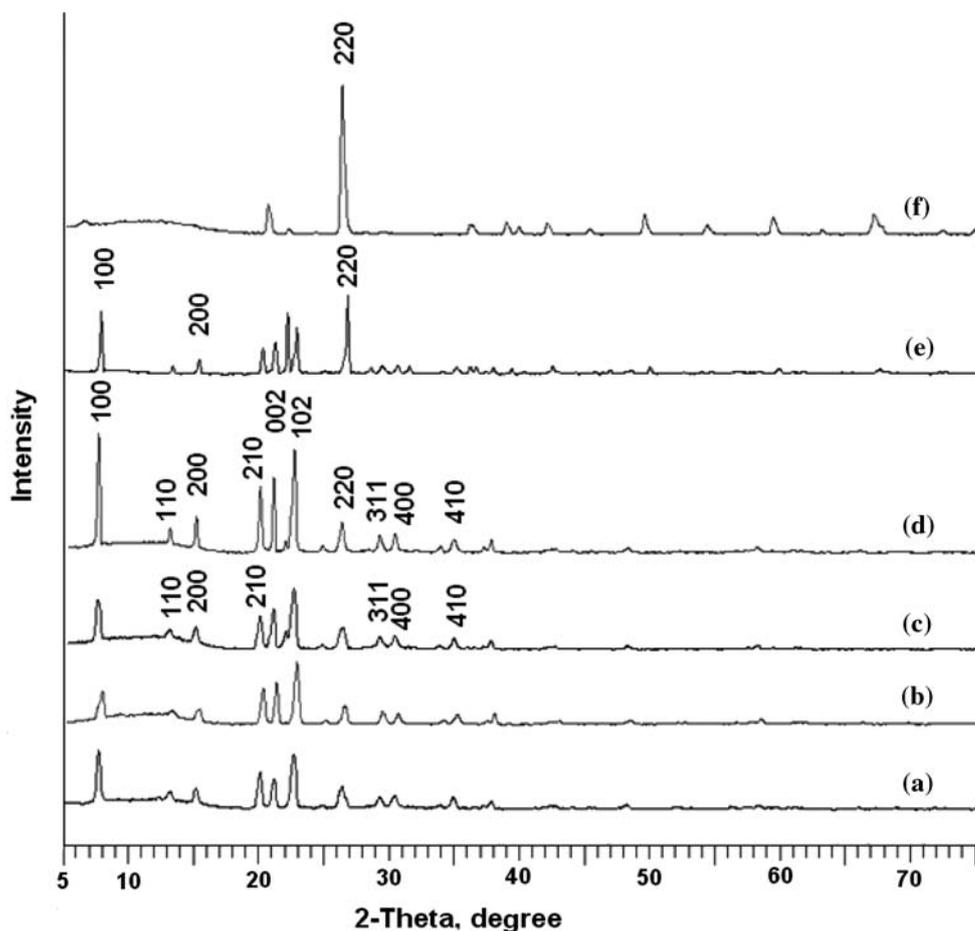
XRD patterns of H5, H6, H7, H8, H9 and H10 were shown in Fig. 7. Diffraction patterns of H5, H6, H7, H8 and H9 correspond to the AFI type structure, similar to those published in the literature [17, 20]. Diffraction pattern of H10 was more likely synthetic berlinite [29] matched with patterns found in XRD software. The intensities of 100, 210, 002 and 102 decreased from H5 to H7, due to the elongation of the crystals [30].

A survey of the literature indicates that a number of additional phases such as $AlPO_4$, boehmite, augelita or $AlPO_4 \cdot 2H_2O$ [17, 31–33] may form during the synthesis of the $AlPO_4$-5 material, depending on the starting gel composition and the synthesis conditions. However, reasons such as small quantities, poor crystallinity, or short-range crystals may explain a weak efficiency of XRD patterns to detect these additional phases. The crystalline form of the natural mineral augelite $Al_2PO_4(OH)_3$, which has a single type of PO_4 tetrahedra and two types of Al polyhedra, i.e., five-coordinated $AlO_2(OH)_3$ and six-coordinated $AlO_4(OH)_2$ were reported was a by-products previously [34, 35].

In the H11 and H12 samples (Fig. 8), ca. 4 µm width and 6 µm length lime type and unreacted crystals formed when the crystallization time was increased to 360 and 420 s respectively at 200 W power exposure. In sample H13 (Fig. 8) angled and longer crystals with narrower ends were examined at 600 s at the same power, whereas in sample H14, at 900 s more incoherent crystals were detected. As the crystallization time was increased from

Fig. 7 XRD patterns of (*a*) H5, (*b*) H6, (*c*) H7, (*d*) H8, (*e*) H9 and (*f*) H10

180 to 900 s, AlPO$_4$-5 crystals began to grow longer and aligned in certain angles. XRD patterns of H11, H12 and H13 were shown in Fig. 8, corresponding to the berlinite structure [29].

The aspect (length-per-width) ratio of the AlPO$_4$-5 crystals varied during synthesizing. The crystals grow mainly in the both *c*-axis and *a*–*b* plane during the first 180 s at 200 W. After 180 s, the crystals did not grow in the *c*-axis any more but in the *a*–*b* plane direction. The ratio of TEA molecules to other chemical species increased at the late stage of the synthesis because phosphate species are consumed faster than TEA in the synthesis mixture [36].

Perfect hexagonal AlPO$_4$-5's formed at 800 W and 60 s crystallization time. It is necessary to heat the starting solution very quickly to the crystallization temperature in order to synthesize pure AlPO$_4$-5 (sample H15, Fig. 8e). When the starting solution is heated slowly, the presence of an amorphous phase indicates incomplete conversion or changing the crystallization behavior, presumably due to slower nucleation and crystallization rates. The perfect crystallites formed in the samples H1, H4 and H15, which has lower crystallization times and enough power in order to form pure AlPO$_4$-5 crystallites.

When second step was added to the AlPO$_4$-5 crystallite formation after 60 s at 800 W the products labeled H16, H17 and H18 were obtained. XRD patterns of H15, H16 and H17, shown in Fig. 9 corresponding to the AFI structure [17, 20], aluminum phosphate structure and berlinite structure [37], respectively. Intensity of the XRD pattern of H17 was higher than that of H18. The second step in the synthesis might have increased the rate of formation of berlinite type of crystals relative to one step syntheses experiments.

The use of microwave heating leads to improved control of the synthesis of molecular sieve crystals. The results showed that the morphology, orientation, and the size of the AlPO$_4$-5 crystals can be controlled by varying the gel composition, water content, and amount of organic template, heating power and crystallization time. Generally, in the microwave heating method, the solution is directly warmed by the dielectric loss of the microwave. The dielectric loss occurs all over the solution. In contrast, in the case of the conventional heating method, the solution is warmed in the autoclave by the conduction of heat. Therefore, using microwave irradiation, the gel is quickly and uniformly heated compared with the conventional
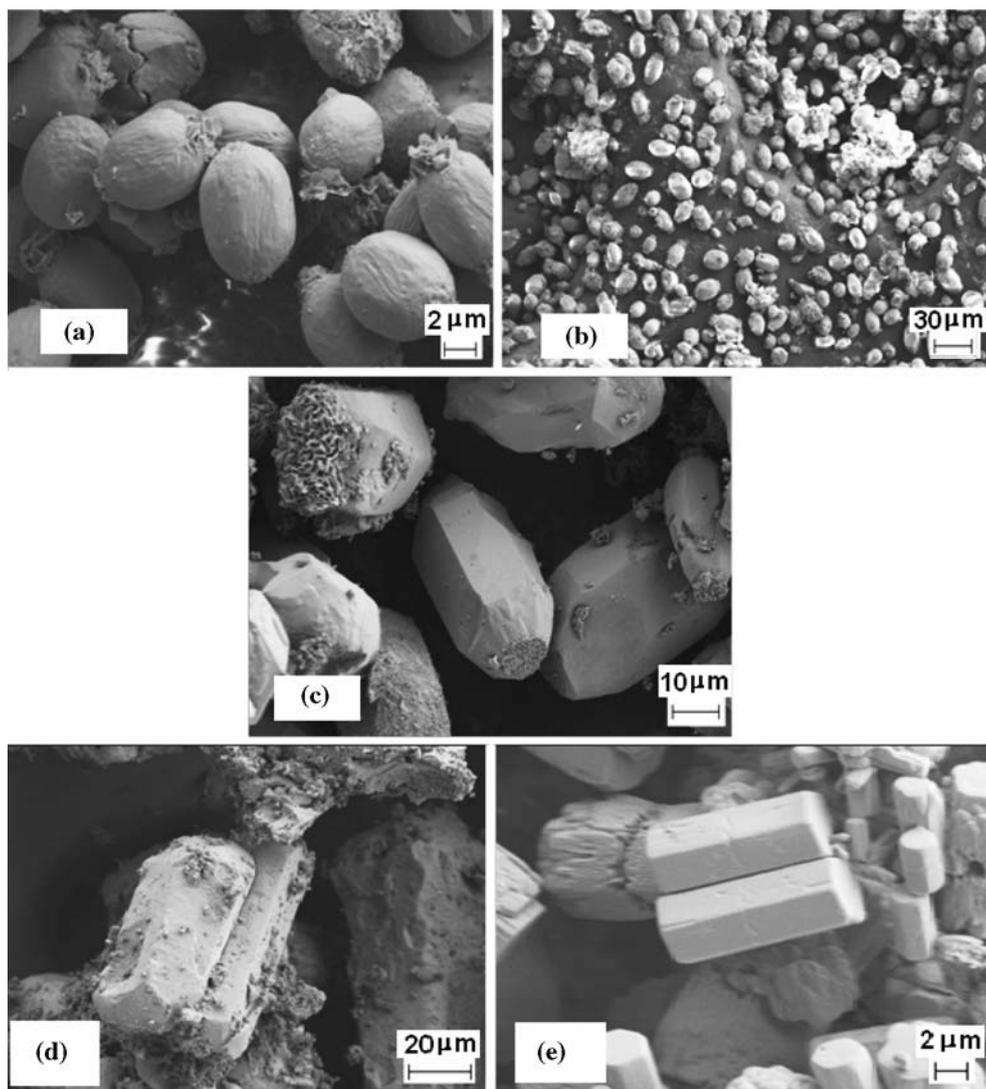
Fig. 8 SEM micrographs of **a** H11, **b** H12, **c** H13, **d** H14 and **e** H15

heating method. For the microwave heating, the temperature over all the gel quickly reaches the condition that starts the reaction. Many crystal nuclei are simultaneously formed all over the gel. Once the nuclei are generated with a high density, the residual Al and P sources are used only for the growth of these nuclei that form crystals. This explains why the crystals have a tendency to have a homogeneous size.

4 Conclusions

In this work, AlPO$_4$-5 with AFI structure containing 12-membered rings was prepared using the aluminum isopropoxide precursor as a source of alumina and TEA as the structure directing agent via microwave technique. It was found that the morphology of the AlPO$_4$-5 depended on the

microwave power and heating time. The influence of the gel composition on the dimensions of AlPO$_4$-5 crystals formed in the system Al$_2$O$_3$:P$_2$O$_5$:(C$_2$H$_5$)$_3$N/or (C$_3$H$_7$)$_3$N):H$_2$O:HF has been studied systematically. A linear correlation between the water content of the reacting gel and both the maximum length and the aspect ratio of the crystals has been found, whereas amine as well as P$_2$O$_5$ contents are controlling the nucleation process. All the AlPO4-5 samples synthesized from the aluminum isopropoxide precursor had only rod-like morphology in a wide range of condition reactions. Crystals with sizes ranging from 10 μm to about 50 μm along the hexagonal c-axis can be synthesized with good yields when these correlations are used. In a two-step synthesis, however, slightly smaller, but very uniform AlPO$_4$-5 crystals with a narrow crystal size distribution without any amorphous or crystalline byproducts could be obtained. Several mechanisms of fast crystallization existed in the
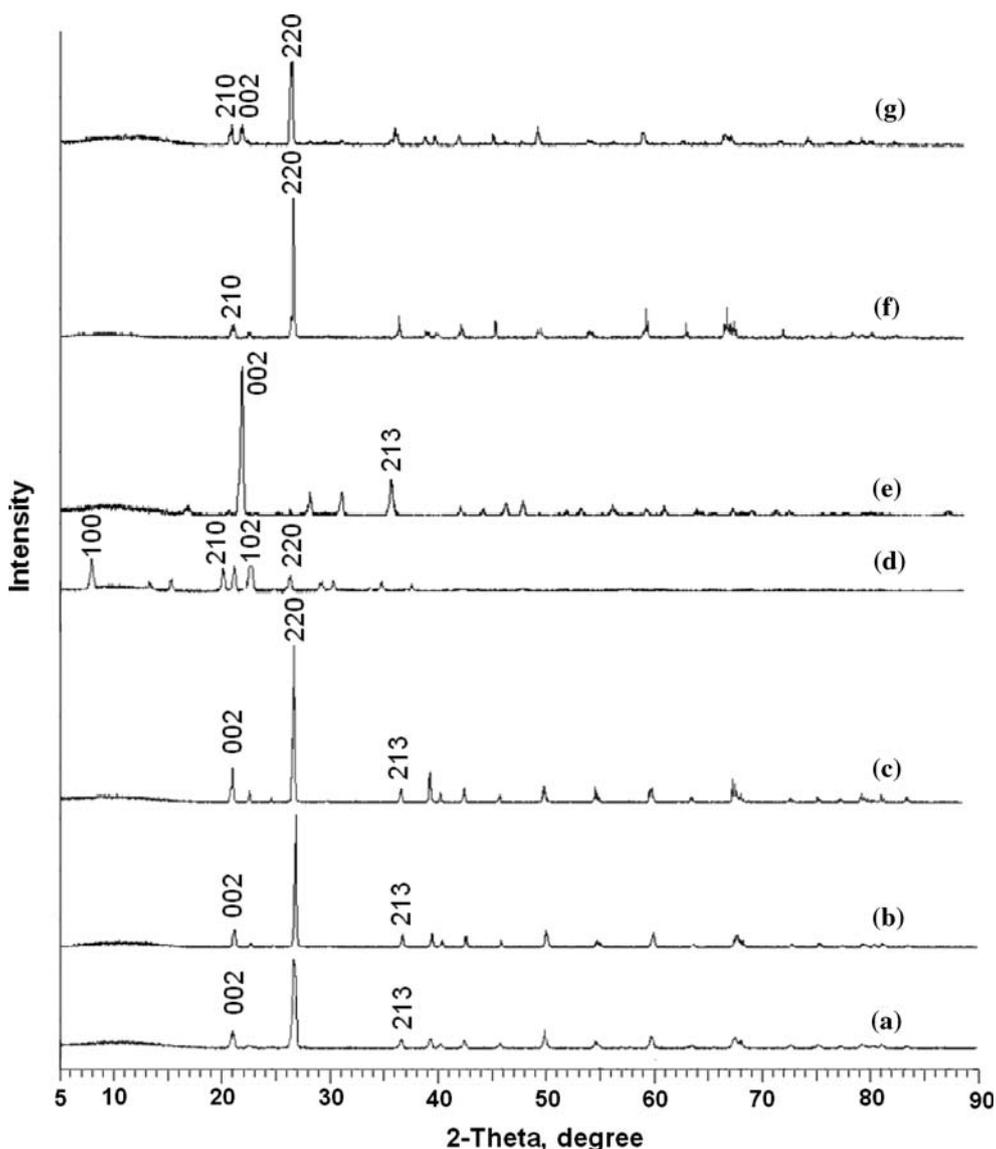
Fig. 9 XRD patterns of (*a*) H11, (*b*) H12, (*c*) H13, (*d*) H15, (*e*) H16, (*f*) H17 and (*g*) H18

microwave radiation, due to increased dissolution of the gel by lonely water molecules in almost temperature gradient-free and convection-free in situ heating. The existence of organic–inorganic arrays as local microassemblies, in these conditions transformed directly into the AFI framework.

References

1. S.H. Lee, P.S. Alegaonkar, J.H. Han, A.S. Berdinsky, D. Fink, Y.-U. Kwon, J.B. Yoo, C.Y. Park, Diam. Relat. Mater. **15**, 1759 (2006)
2. M.E. Davis, Nature **417**, 813 (2002)
3. Z.X. Chang, R. Koodali, R.M. Krishna, L. Kevan, J. Phys. Chem. B **104**, 5579 (2000)
4. B. Paizs, E. Tajkhorshid, S. Suhai, J. Phys. Chem. B **103**, 5338 (1999)
5. L. Domokos, L. Lefferts, K. Seshan, J.A. Lerchery, J. Catal. **203**, 351 (2001)
6. M. Höchtl, A. Jentys, H. Vinek, Appl. Catal. A **207**, 397 (2001)
7. S.C. Laha, G. Kamalakar, R. Glaser, Micropor. Mesopor. Mater. **90**, 45 (2006)
8. S.H. Jhung, J.-S. Chang, J.S. Hwang, S.-E. Park, Micropor. Mesopor. Mater. **64**, 33 (2003)
9. G. Tompsett, W.C. Conner, K.S. Yngvesson, Chem. Phys. Chem. **7**, 296 (2006)
10. H.B. Du, M. Fang, W.G. Xu, X.P. Meng, W.Q. Pang, J. Mater. Chem. **7**, 551 (1997)
11. M. Fang, H.B. Du, W.G. Xu, X.P. Meng, W.Q. Pang, Micropor. Mater. **9**, 59 (1997)
12. I. Braun, G. Schulz-Ekloff, D. Wohrle, W. Lautenschlager, Micropor. Mesopor. Mater. **23**, 79 (1998)

13. H.J. Sung, J.S. Chang, S.H. Jin, E.P. Sang, Micropor. Mesopor. Mater. **64**, 33 (2003)
14. M. Sathupunya, E. Gulari, S. Wongkasemjit, Mater. Chem. Phys. **83**, 89 (2004)
15. H.J. Sung, W.Y. Ji, K.H. Young, S.C. Jong, Micropor. Mesopor. Mater. **89**, 9 (2006)
16. Y.K. Hwang, J.S. Chang, Y.U. Kwon, S.E. Park, Stud. Surf. Sci. Catal. **146**, 101 (2003)
17. S. Qiu, Q. Piang, H. Kessler, J.L. Guth, Zeolites **9**, 440 (1989)
18. G. Finger, J. Richter-Mendav, M. Bulow, J. Kornatowski, Zeolites **11**, 443 (1991)
19. I. Girnus, K. Jancke, R. Vetter, J. Richter-Mendau, J. Caro, Zeolites **15**, 33 (1995)
20. S. Mintova, S. Mo, T. Bein, Chem. Mater. **10**, 4030 (1998)
21. J.W. Richardson Jr., J.J. Pluth, J.V. Smith, Acta Crystallogr. **C43**, 1469 (1987)
22. T. Ikeda, K. Miyazawa, F. Izumi, Q. Huang, A. Santoro, J. Phys. Chem. Solids **60**, 1531 (1999)
23. K. Utchariyajit, S. Wongkasemjit, Micropor. Mesopor. Mater. **114**, 175 (2008)
24. D. Demuth, G.D. Stucky, K. Unger, F. Schüth, Micropor. Mater. **3**, 473 (1995)
25. G.J. Klap, H. van Koningsveld, H. Graafsma, A.M.M. Schreurs, Micropor. Mesopor. Mater. **38**, 403 (2000)
26. A. Iwasaki, T. Sano, T. Kodaira, Y. Kiyozumi, Micropor. Mesopor. Mater. **64**, 145 (2003)
27. J.-C. Lin, J.T. Dipre, M.Z. Yates, Langmuir **20**, 1039 (2004)
28. U. Vietze, O. Krauss, F. Laeri, G. Ihlein, F. Schuth, B. Limburg, M. Abraham, Phys. Rev. Lett. **81**, 4628 (1998)
29. N. Thong, D. Schwarzenbach, Acta Crystallogr. **53**, 35 (1979)
30. S.H. Jhung, J.-S. Chang, D.S. Kim, S.-E. Park, Micropor. Mesopor. Mater. **71**, 135 (2004)
31. E. Jahn, D. Müller, W. Wieker, J. Richter-Mendau, Zeolites **9**, 177 (1989)
32. A.N. Christensen, T.R. Jensen, P. Norby, J.C. Hanson, Chem. Mater. **10**, 1688 (1998)
33. G.S. Zhu, F.S. Xia, S.L. Qui, P.C. Hun, R.R. Xu, S.J. Ma, O. Terasaki, Micropor. Mater. **11**, 269 (1997)
34. D.R. Gougeon, B.E. Brouwer, R.B. Philippe, L. Delmotte, C. Marichal, J.M. Chezeau, R.K. Harris, J. Phys. Chem. B **105**, 12249 (2001)
35. T. Araki, J.J. Finney, T. Zoltai, Am. Mineral. **53**, 1096 (1968)
36. T. Kodaira, K. Miyazawa, T. Ikeda, Y. Kiyozumi, Micropor. Mesopor. Mater. **29**, 329 (1999)
37. R.C.L. Mooney, Acta Crystallogr. **9**, 728 (1956)